A note on the local behavior of the Taylor method for stiff ODEs

Philip P. Forrier[(1,*)] Joan Gimeno[(1)] Àngel Jorba[(1,2)]

July 17, 2024

(1) Departament de Matemàtiques i Informàtica, Universitat de Barcelona, Gran Via de les Corts Catalanes, 585, 08007 Barcelona, Spain, {philip,joan,angel}@maia.ub.es

(2) Centre de Recerca Matemàtica (CRM), Edifici C, Campus UAB, 0 Floor, 08193 Bellaterra, Barcelona, Spain

* corresponding author

Abstract

In this note we study the behavior of the coefficients of the Taylor method when computing the numerical solution of stiff Ordinary Differential Equations. First, we derive an asymptotic formula for the growth of the stability region w.r.t. the order of the Taylor method. Then, we analyze the behavior of the Taylor coefficients of the solution when the equation is stiff. Using jet transport, we show that the coefficients computed with a floating point arithmetic of arbitrary precision have an absolute error that depends on the variational equations of the solution, which can have a dominant exponential growth in stiff problems. This is naturally related to the characterization of stiffness presented by Söderlind *et al.* and allows to discuss why explicit solvers need a stepsize reduction when dealing with stiff systems. We explore how high-order methods can alleviate this restriction when high precision computations are required. We provide numerical experiments with classical stiff problems and perform extended precision computations to demonstrate this behavior.

2010 Mathematics Subject Classification. 34A34, 34A45, 65L04, 65L05, 65L20, 65L70

Keywords: Stiff Ordinary Differential Equations; Stiff Systems; Stiffness Indicator; Taylor Method; Jet Transport; Extended Precision; Optimal Order; Step Size

Contents

1. Introduction

Ordinary Differential Equations (ODEs) are fundamental in modeling a wide range of physical, biological, and engineering systems. In practice, an ODE is often recognized as stiff due to the poor performance of explicit numerical methods, which require excessively small stepsizes to maintain stability. This limitation is traditionally mitigated by using implicit methods that require to solve an equation at each step, albeit at a higher computational cost. Despite the practical recognition of stiffness, there is no consensus on its formal definition and detection. Efforts to characterize stiffness typically involve examining properties of the problem that differ vastly in magnitude, such as eigenvalues, pseudospectra, norms, or Lipschitz constants [SJC15].

The Taylor method is the paradigm of high-order solvers, which achieve high accuracy by increasing the order of the method without the need of stepsize reductions. It is, in fact, the method of choice for extended accuracy integrations [JZ05, ABBR12], that is, using a multiple precision arithmetic. However, being an explicit method, it may not be suitable for highly stiff problems. Other alternative high-order approaches, such as Hermite-Obreschkoff methods [CGH$^+$97, Ned99] or implicit Taylor methods [KC92], have been developed for validated integration of stiff equations. Another recent option is the use of Padé approximants [Amo22]. Given that the Taylor method is the core of all these high order approaches, understanding its behavior when applied to stiff equations becomes crucial.

Usually, a rapid growth of the Taylor coefficients indicates that there is a nearby singularity of the solution, possibly for complex time, which requires a reduction of the stepsize (there are some strategies that allow for stepsizes larger than the radius of convergence [CC82]). This is not considered stiff.

Let us consider the case in which the solution has a strongly attracting direction of exponential type with parameter λ large and negative. Roughly speaking, the n-th degree term of the Taylor series of the solution contains $\lambda^n/n!$, which grows until $n \approx |\lambda|$. If floating point arithmetic were exact and the Taylor series were of sufficiently high order, the contribution of these terms would be small for any stepsize h. However, if the order of the Taylor series is not high enough, the stepsize has to be drastically reduced due to the large Taylor coefficients. As extended precision integrations require higher orders, problems that are stiff with double precision can turn out to be non-stiff for high accuracy integrations. In this note, we analyze the behavior of these coefficients and the conditions under which an efficient and extended precision Taylor method can be used for moderately stiff equations.

The paper is organized as follows: Section 1.1 contains a brief review of the Taylor method and jet transport, followed in Section 1.2 by a summary of the logarithmic norm [Söd06] and the stiffness indicator presented in [SJC15]. Section 2 studies the growth of the stability region of the Taylor method. Section 3 studies the behavior of the Taylor coefficients by using a jet transport technique. Finally, Section 4 illustrates this study by providing numerical experiments for some stiff systems and reports extended precision computations of the period and amplitude of the van der Pol oscillator.

1.1 The Taylor method

The Taylor method is one of the oldest methods for the numerical integration of Initial Value Problems (IVP),

$$y'(x) = f(x, y(x)), \quad y(x_0) = y_0, \tag{1}$$

where $f\colon \mathbb{R} \times \mathbb{R}^N \to \mathbb{R}^N$ is a sufficiently smooth function. The Taylor method is based on the computation of the Taylor series of the solution. One step of the method of order n with stepsize h is

$$y_1 = y_0 + {y_0}^{[1]} h + \cdots + {y_0}^{[n]} h^n, \tag{2}$$

where ${y_0}^{[k]}$ denotes the normalized derivative of the solution w.r.t. x at x_0; that is,

$${y_0}^{[k]} = \frac{1}{k!}\frac{d^k}{dx^k}[y(x)](x_0) = \frac{1}{k!}\frac{d^{k-1}}{dx^{k-1}}[f(x, y(x))](x_0, y_0).$$

The use of automatic differentiation for computing the coefficients $\{y_0^{[k]}\}_k$ has led to very efficient implementations, allowing to achieve arbitrarily high orders n [JZ05, ABBR12, GJZ22]. Another application of automatic differentiation is to replace the floating point arithmetic on a numerical integrator by an arithmetic of truncated power series with floating point coefficients (see [GJJ+23]). This technique, called 'jet transport', is used for the efficient integration of variational equations of arbitrary order for the IVP (1). The main theorem in this context is the following:

Theorem 1.1 ([GJJ+23])**.** *Given a step size h, the use of jet transport of order m on a Runge–Kutta method, Taylor method or multistep method produces exactly the same results as the integration of variational equations up to order m with the same integration method.*

The theorem provides a theoretical framework to reliably compute high-order derivatives of the flow, which naturally appear in different kinds of settings. Recently, [For23] has extended Theorem 1.1 to General Linear methods. A particular case are the first variational equations,

$$\begin{aligned} y'(x) &= f(x, y(x)) \ , & y(x_0) &= y_0, \\ V'(x) &= \mathrm{D}_y f(x, y(x)) V(x) \ , & V(x_0) &= I \ , \end{aligned} \tag{3}$$

where, being $\Phi(x; x_0, y_0)$ the flow at time x of the IVP (1), $V(x) \coloneqq \mathrm{D}_{y_0}\Phi(x; x_0, y_0)$, and I is the identity matrix of size N.

In order to develop strategies for the choice of order and stepsize of the Taylor method, it is customary to assume properties about the analyticity of the solution $y(x)$ [Sim01, JZ05]. This has been used to determine estimates for optimal stepsize h_{opt} and order n_{opt} in the following sense:

Theorem 1.2. *Assume that the function $h \mapsto y(x_0 + h)$ is analytic on a disk of radius ρ. Let C be a positive constant such that*

$$\|y_0^{[k]}\| \leqslant C/\rho^k, \qquad \forall k \in \mathbb{N}.$$

Then, if the required accuracy ε tends to 0, the values of h and n that give the required accuracy and minimize the global number of operations tend to

$$n_{\text{opt}} = -\frac{1}{2}\log\Big(\frac{\varepsilon}{C}\Big) - 1, \qquad h_{\text{opt}} = \frac{\rho}{e^2}.$$

In practice, the optimal values are usually approximated by

$$n_{\text{opt}} = \left\lceil -\frac{1}{2}\log\varepsilon + 1 \right\rceil, \qquad h_{\text{opt}} = \frac{1}{e^2} \cdot \min\left\{ \left(\frac{\max\{1, \|y_0\|\}}{\|y_0^{[n_{\text{opt}}]}\|} \right)^{1/n_{\text{opt}}}, \left(\frac{\max\{1, \|y_0\|\}}{\|y_0^{[n_{\text{opt}}-1]}\|} \right)^{1/(n_{\text{opt}}-1)} \right\},$$

which ensure that the contribution of order $n_{\text{opt}} - 1$ is lower than ε, and that of order n_{opt} is lower than ε/e^2 [JZ05]. It is common to multiply h_{opt} by a safety factor of the form $\exp(-0.7/(n_{\text{opt}} - 1))$.

1.2 The stiffness indicator

As Hairer and Wanner note, "stiff equations are problems for which explicit methods don't work" [HW96]. The Taylor method is no exception, as it "is not suitable for stiff equations, because, in this case, the errors can grow too fast" [JZ05]. Recently, Söderlind, Jay and Calvo [SJC15] have defined an indicator for stiffness that is highly compatible with jet transport, as it is "based on sharp short-term bounds on perturbation growth and decay rates in the variational equations". This indicator is computable from the logarithmic norm, which is defined as follows:

Definition 1.3 ([Söd06])**.** The logarithmic norm of a matrix A is

$$\mu(A) = \lim_{h \to 0^+} \frac{\|I + hA\| - 1}{h}.$$

As explained in [Söd06], it was introduced as a topological condition on A to guarantee the boundedness of the solutions of the linear system $v'(x) = Av(x)$, because the norm of $v(x)$ satisfies

$$\mathrm{D}^+\|v(x)\| \leqslant \mu(A)\|v(x)\|,$$

where D^+ denotes the upper right Dini derivatives. An analogous bound is derived by the change of variable $x \to -x$. Integrating these inequalities yields, for $x \geqslant x_0$, the perturbation bound

$$\|v(x_0)\|e^{-x\mu(-A)} \leqslant \|v(x)\| \leqslant \|v(x_0)\|e^{x\mu(A)}.$$

This notion was then extended to the space of Lipschitz maps in terms of the *least upper bound* (lub) logarithmic Lipschitz constant $M(\cdot)$ (for a matrix A, $M(A) = \mu(A)$). With this definition, the analysis can be extended to the linear system

$$v'(x) = A(x)v(x),$$

where analogous bounds on the norm of $v(x)$ hold by replacing $\mu(A)$ by $M(A(x))$. Again, integration yields the bounds (see [Cop65, p. 58])

$$\|v(x_0)\| \exp\left(\int_{x_0}^{x} m(A(s))\,ds\right) \leqslant \|v(x)\| \leqslant \|v(x_0)\| \exp\left(\int_{x_0}^{x} M(A(s))\,ds\right), \tag{4}$$

where $m(f) \coloneqq -M(-f)$ is the *greatest lower bound* (glb) logarithmic Lipschitz constant. Under these considerations, the stiffness indicator presented in [SJC15] is

$$\sigma(A) = \tfrac{1}{2}(m(A) + M(A)), \tag{5}$$

and as stated, "a necessary condition for stiffness is that $\sigma(\mathrm{D}_y f(x, y(x)))$ is 'large' and negative". A remarkable property of this stiffness indicator is that it is easy to compute. For the most common norms $\|\cdot\|_\infty$, $\|\cdot\|_1$ and $\|\cdot\|_2$, if A is a matrix with entries a_{ij}, $\Re(\cdot)$ denotes the real part of a complex number, and $\Lambda(\cdot)$ the set of eigenvalues of a matrix, then (see [Cop65])

$$\mu_\infty(A) = \max_i\big(\Re(a_{ii}) + \sum_{j,j\neq i} |a_{ij}|\big), \quad \mu_1(A) = \max_j\big(\Re(a_{jj}) + \sum_{i,i\neq j} |a_{ij}|\big), \quad \mu_2(A) = \max \Lambda\big(\tfrac{1}{2}(A + A^T)\big).$$

2. Asymptotic growth of the stability region

Studying the growth of the stability region of the Taylor method, Barrio *et al.* [BBL05] computed a linear fit up to order 60 of the real stability abscissae, and Ketcheson *et al.* [KLK15] provided disks that enclose or are enclosed by the stability region.

Our approach will be to derive an explicit asymptotic formula for the growth of the real stability abscissae of the stability regions in terms of the order of the Taylor method, which will be proven useful in Section 3 to characterize stability restrictions.

Definition 2.1 ([HW96])**.** The stability region of a one-step method is the set

$$\mathcal{S} = \{z \in \mathbb{C} \ ; \ |R(z)| \leqslant 1\},$$

where the stability function $R(\cdot)$ is the numerical solution ($y_1 = R(h\lambda)y_0$) after one step for the Dahlquist test equation

$$y' = \lambda y, \quad y_0 = 1. \tag{6}$$

Definition 2.2 ([HW96])**.** A method is called A-stable if its stability domain $\mathcal{S}$ contains the complex left-half plane; that is, if

$$\mathcal{S} \supset \mathbb{C}^- \coloneqq \{z \in \mathbb{C} \ ; \ \Re(z) \leqslant 0\}.$$

It follows then that the stability function of the Taylor method of order n is no other but the partial sum (section) of the power series of $\exp(z)$,

$$s_n(z) = \sum_{k=0}^{n} \frac{z^k}{k!}.$$

It is well known [HW96] that A-stability is a desirable property when dealing with stiff problems. Unluckily, as most explicit methods, the Taylor method (for finite order n) is not A-stable [BBL05]. For that reason, we are interested in the growth on the complex left-half plane $\mathbb{C}^-$ of the stability region $\mathcal{S}_n$ with respect to the order of the method (let us specify the Taylor order n in the name of $\mathcal{S}$). For that, we will study in particular the growth of the interval

$$[-\ell_n, 0] \coloneqq \mathcal{S}_n \cap \mathbb{R}^-,$$

where $\mathbb{R}^- \coloneqq \mathbb{R} \cap \mathbb{C}^-$ is the negative real axis and the values $\ell_n \geqslant 0$ are usually referred to as real stability abscissae. For that, we note that the boundary of $\mathcal{S}_n$ is given by the zeros of $s_n(z) - \alpha$ for some $\alpha \in \mathbb{S}^1$, which are exactly the zeros of the sections of $\exp(z) - \alpha$, studied by Dieudonné [Die35]. According to the following theorem of Cauchy,

Lemma 2.3 ([GG14])**.** *If $\sum_{k=0}^{n} a_k z^k$ is a polynomial of degree n with coefficients $a_k \in \mathbb{C}$, then all its zeros lie in*

$$|z| \leqslant 1 + \max_{0 \leqslant k \leqslant n-1} |a_k/a_n|.$$

The zeros of $s_n(z) - \alpha$ are then in the region $|z| \leqslant 1 + 2n!$, while the zeros of the normalized sections $s_n(nz) - \alpha$ will all lie in $|z| \leqslant 2$, therefore easing their study.

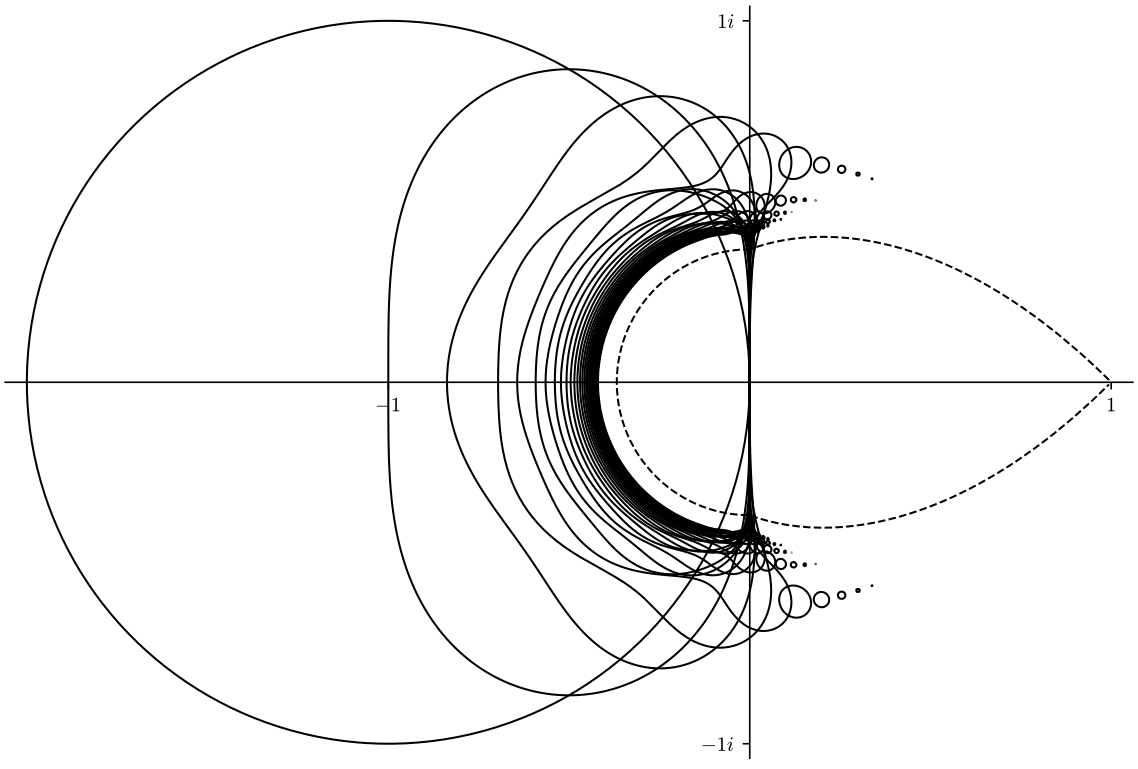

Figure 1: *Boundary of the scaled stability regions $n\mathcal{S}_n$*, for orders 1 to 30 (solid) and the limiting set of the zeros of the sections of $\exp(z) - \alpha$ (dashed).

In this context, Dieudonné proved that the zeros of $s_n(nz) - \alpha$ with negative real part have as limit points the circle $|z| = 1/e$, the zeros with positive real part approach the so-called Szegő curve $\left|ze^{1-z}\right| = 1$ and the zeros that actually approximate the zeros of $\exp(z) - \alpha$ lie in the segment $[-\boldsymbol{i}/e, \boldsymbol{i}/e]$. A visual study of the scaled stability regions $n\mathcal{S}_n = \{z \in \mathbb{C} \ ; \ |s_n(nz)| \leqslant 1\}$ reveals this behavior (see

Figure 1). We stress that the relation between $\mathcal{S}_n$ and $n\mathcal{S}_n$ is a simple multiplication by n, and the same relation will hold for the zeros of their stability functions.

With this in mind, we derive in Theorem 2.4 an asymptotic expression for the growth of the real stability abscissae ℓ_n in terms of the real zeros of $s_n(nz) - \alpha$, similar to the one derived by Szegő for $s_n(nz)$ [Zem05]. We also explore the conclusion of Rosenbloom [Ros42] (see also [Var12]) that the zeros of the section of order n of an entire function of positive finite order, $\sum_{k=0}^{n} a_k z^k$, grow as $|a_n|^{-1/n}$.

Theorem 2.4. *The real stability abscissae ℓ_n of $\mathcal{S}_n$ grows asymptotically as*

$$\ell_n = \frac{n}{e} + \frac{1}{e} \cdot \log\left(\sqrt{2\pi n}(1+e)\right) + \mathcal{O}\left(\frac{\log^2 n}{n}\right), \tag{7}$$

which can also be expressed in terms of

$$\ell_n = (n!)^{1/n} + \frac{1}{e}\log(1+e) + \mathcal{O}\left(\frac{\log^2 n}{n}\right). \tag{8}$$

Proof. Choosing $\alpha = (-1)^n \in \mathbb{R}$, we ensure that $s_n(z) - \alpha$ has a unique (nonzero) negative real zero. This follows from the fact that every real polynomial of odd degree has at least one real zero so, for odd n, $s_n(z)+1$ has at least a real zero different from zero and, for even n, the same holds for $s_n(z)-1$, as it can be factored as z times a real polynomial of odd degree. Being $(s_n(z) - \alpha)' = s_{n-1}(z)$, as $s_k(z)$ has exactly one real root for odd k and none for even k (see [Zem05, Proposition 2]), by Rolle's theorem, $s_n(z) - \alpha$ has at most 1 real root for even n and at most 2 for odd n. In addition, the (nonzero) real zero is negative by Descartes' rule of signs.

It then follows from the work of Dieudonné [Die35, p. 341] that $s_n(nz) - \alpha = 0$ is equivalent to

$$\frac{\alpha}{(ze)^n} = \frac{1}{\sqrt{2\pi n}} \cdot \frac{z}{1-z} \cdot (1 + \mathcal{O}(1/n)).$$

Then, as the zeros of $s_n(nz) - \alpha = 0$ in $\mathbb{C}^-$ converge to $|z| = 1/e$, consider $z = -1/e - \delta$ with $\delta \sim 0$. Taking logarithms, dividing by n and expanding at $\delta = 0$, we obtain

$$-e\delta + \mathcal{O}(\delta^2) = -\frac{1}{n}\log\left(\sqrt{2\pi n}\right) - \frac{1}{n}\log(1+e) + \mathcal{O}\left(\frac{\delta}{n}\right) + \mathcal{O}\left(\frac{1}{n^2}\right),$$

and so δ is of the form

$$\delta = \frac{1}{e} \cdot \frac{1}{n}\log\left(\sqrt{2\pi n}(1+e)\right) + \mathcal{O}\left(\frac{\log^2 n}{n^2}\right).$$

The first part follows by noting that, by construction, $\ell_n/n = 1/e + \delta$. For the second, as (see [Nem10])

$$\begin{aligned}
\frac{1}{n}(n!)^{1/n} &= \frac{1}{n}\left(\sqrt{2\pi n}(n/e)^n(1+\mathcal{O}(1/n))\right)^{1/n} = \frac{1}{e}\exp\left(\frac{\log(2\pi n)}{2n}\right)(1+\mathcal{O}(1/n))^{1/n} \\
&= \frac{1}{e}\left(1 + \frac{\log(2\pi n)}{2n} + \mathcal{O}\left(\frac{\log^2(n)}{n^2}\right)\right)(1+\mathcal{O}(1/n))^{1/n} \\
&= \frac{1}{e} + \frac{1}{e}\cdot\frac{1}{n}\log\left(\sqrt{2\pi n}\right) + \mathcal{O}\left(\frac{\log^2(n)}{n^2}\right),
\end{aligned}$$

comparison with the expansion derived on the fist part yields the result. □

In Figure 2 we show the error of the approximations to ℓ_n of Theorem 2.4 and compare them with the error of the linear approximation $\ell_n \approx 1.3614 + 0.3725n$ of Barrio *et al.* [BBL05]. This linear approximation has the smallest error up to order $n \approx 60$, for which it was devised. For higher orders, it is improved by the asymptotic expressions of Theorem 2.4, since their errors decrease steadily. In particular, we observe that (8) appears to perform slightly better than (7).

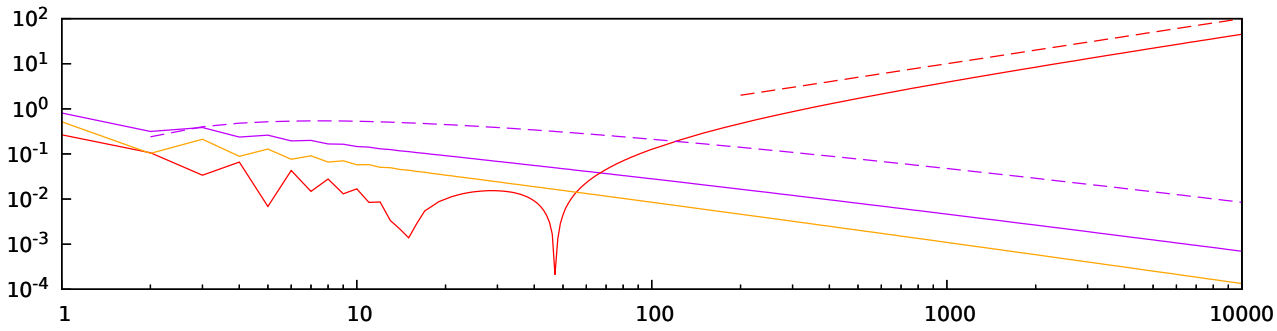

Figure 2: *Absolute error of the approximations to the real stability abscissae* ℓ_n. We show from top to bottom on the right-hand side, in solid lines, the errors with respect to the order n of the approximation in [BBL05] (red), of the expansion (7) (purple) and of the expression (8) (orange). We also display in dashed lines and in the same order the growth of $0.01 \cdot n = \mathcal{O}(n)$ (red) and $\mathcal{O}(\log^2(n)/n)$ (purple).

3. Behavior of the finite precision jet of derivatives

The jet of normalized derivatives $\{{y_0}^{[k]}\}_k$ is computed recursively at each step of the Taylor method from an initial value y_0. However, the use of a floating point arithmetic with unit roundoff u induces an error $|\varepsilon| \leqslant u$, so that the initial value is effectively

$$\widehat{y}_0 = y_0 + \varepsilon v_0, \tag{9}$$

where v_0 is an arbitrary norm-one vector of the same dimension of y_0. To study the propagation of this error on the coefficients ${y_0}^{[k]}$ (see also [Chr92, GKW12, RB12]), we consider ε a symbol and expand around y_0,

$$\widehat{y}_0{}^{[k]} = \frac{1}{k!}\frac{d^{k-1}}{dx^{k-1}}[f(x,y(x))](x_0,\widehat{y}_0) = {y_0}^{[k]} + \varepsilon\frac{1}{k!}\frac{d^{k-1}}{dx^{k-1}}[\mathrm{D}_y f(x,y(x))](x_0,y_0)v_0 + \mathcal{O}(\varepsilon^2).$$

Let us drop higher orders of ε, which are briefly discussed in Section 3.2. Therefore, as proved by Gimeno *et al.* [GJJ+23], this is no other but the use of jet transport of order 1 with 1 symbol, and so it is equivalent to the computation of the Taylor coefficients of the first variational equations (3) in the direction v_0. To simplify the exposition, we follow the notation

$$\widehat{y}_0{}^{[k]} = {y_0}^{[k]} + \varepsilon {v_0}^{[k]}. \tag{10}$$

Depending on the behavior of ${y_0}^{[k]}$ and ${v_0}^{[k]}$ with respect of the order k, there may exist some 'effective' order n_{eff} for which the leading term is that of the error; that is,

$$\|{y_0}^{[k]}\| \ < \varepsilon \|{v_0}^{[k]}\| \qquad \text{for} \qquad k > n_{\text{eff}}. \tag{11}$$

In that case, the use of the values $\widehat{y}_0{}^{[k]}$ for $k > n_{\text{eff}}$ could be inappropriate. If n_{eff} is smaller than the desired order for the method, this could affect the performance of usual strategies for order and stepsize control. Given the nature of the Taylor method, it is not surprising that a restriction on the achievable order is harmful. Let us recall that "methods whose order is not very high can be extremely slow for computations requiring extended precision arithmetic. Note that the Taylor method does not need to reduce the stepsize to increase accuracy; it can increase the order" [JZ05].

To study this, observe that the bounds (4) applied to $v(x)$ for $x_0 \leqslant x \leqslant x_0 + h$ are

$$\exp\left(\int_{x_0}^{x} m(\mathrm{D}_y f(s,y(s)))\,ds\right) \leqslant \|v(x)\| \leqslant \exp\left(\int_{x_0}^{x} M(\mathrm{D}_y f(s,y(s)))\,ds\right),$$

so we consider some function $\lambda(x)$ satisfying $m(\mathrm{D}_y f(x,y(x))) \leqslant \lambda(x) \leqslant M(\mathrm{D}_y f(x,y(x)))$ such that $\|v(x)\| = \exp\left(\int_{x_0}^{x} \lambda(s)ds\right)$. For h small, $\int_{x_0}^{x} \lambda(s)ds = \lambda(x_0)(x-x_0) + \mathcal{O}((x-x_0)^2)$ for $x_0 \leqslant x \leqslant x_0 + h$, and so we only consider first order terms in $\lambda(x)$. Let us stress that the stiffness indicator is devised as

a characterization of the behavior above, thus making $\lambda(x_0) \approx \sigma(\mathrm{D}_y f(x_0, y(x_0))$ a reasonable choice. Henceforth, we assume that the norm of the coefficients of $v(x)$ are well represented by

$$\|{v_0}^{[k]}\| = \frac{|\sigma|^k}{k!}, \tag{12}$$

where we denote $\sigma \coloneqq \sigma(\mathrm{D}_y f(x_0, y(x_0)))$ for simplicity. This assumption on the behavior of the variational equations is verified in the numerical experiments of Section 4 for the van der Pol oscillator and the Oregonator models in the regions of stiffness; that is, where σ is large and negative. We observe that a more conservative approach would be to choose $\lambda(x_0) \approx m(\mathrm{D}_y f(x_0, y(x_0)))$, which is already a necessary condition for stiffness [SJC15]. Let us therefore study the consequences of the computed coefficients behaving as

$$\|{\widehat{y}_0}^{[k]}\| = \|{y_0}^{[k]}\| + \varepsilon\frac{|\sigma|^k}{k!}. \tag{13}$$

where we find worth noting the similarity with the synthesized stiff problem of Chang [Cha89].

3.1 Truncation error of the floating point solution

To derive strategies for the control of the stepsize h and order n of the Taylor method (see [Sim01, JZ05, ABBR12, RB12]), it is usual to resort to the study of the truncation error

$$\|y(x_0 + h) - y_1\| \leqslant \texttt{tol},$$

where $y(x_0 + h)$ denotes the exact solution of the IVP (1), y_1 is the step of the Taylor method as in (2) and `tol` is some desired tolerance commonly chosen smaller than the unit roundoff.

Not being usual in the literature to consider the effects of (11), most error estimators implicitly assume the same behavior for the coefficients of the exact and numerical solutions, neglecting floating point errors of the section of the series. To study these effects for a method of order n, we consider the difference of the exact solution of order $n + 1$ and the floating point solution of order n

$$\left\|\sum_{k=0}^{n+1} {y_0}^{[k]} h^k - \sum_{k=0}^{n} {\widehat{y}_0}^{[k]} h^k\right\| = \left\|{y_0}^{[n+1]} h^{n+1} - \sum_{k=0}^{n} \varepsilon {v_0}^{[k]} h^k\right\| \leqslant \texttt{tol}.$$

Notice that when the rounding error is negligible, this estimator is of the order of the term $n + 1$ of the series. However, for the case of (12), the estimator under the triangular inequality becomes

$$\left\|{y_0}^{[n+1]} h^{n+1}\right\| + \left\|\sum_{k=0}^{n} \varepsilon \frac{\sigma^k}{k!} h^k\right\| = \left\|{y_0}^{[n+1]}\right\| h^{n+1} + \varepsilon |s_n(\sigma h)| \leqslant \texttt{tol}, \tag{14}$$

where s_n is the stability function of the Taylor method of order n, as in Section 2.

If $|s_n(\sigma h)| \leqslant 1$, this terms has no effect, and the selection of stepsize and order can be simply based on the behavior of the normalized derivatives. Otherwise, to control the truncation error, restrictions must be applied to ensure $|s_n(\sigma h)| \leqslant 1$. In this last case, notice that the solution of the IVP is restricted by the stability of the Dahlquist test equation (6) with parameter σ and initial condition $y_0 = \varepsilon$.

3.1.1 Stability through stepsize reduction

The most common approach to satisfy the restriction $|s_n(h\sigma)| \leqslant 1$ is to reduce the stepsize. We observe that, in particular, stepsize selection strategies for the Taylor method that are based on the study of the last coefficient, when applied to the floating point coefficients, satisfy this restriction. That is, if the error estimator is based on the study of $\|{\widehat{y}_0}^{[n]}\| \, h^n \leqslant \texttt{tol}$ (see [ABBR12]), the stepsize satisfies

$$h = \left(\frac{\texttt{tol}}{\|{\widehat{y}_0}^{[n]}\|}\right)^{1/n} \leqslant \left(\frac{\texttt{tol}}{\varepsilon|\sigma|^n/(n!)}\right)^{1/n} \leqslant \left(\frac{\texttt{tol}}{\varepsilon}\right)^{1/n} \frac{1}{|\sigma|}(n!)^{1/n}.$$

It follows from Theorem 2.4 that, for $\texttt{tol} \leqslant \varepsilon$, being $h|\sigma| = \mathcal{O}(\ell_n)$, the stepsize is restricted by the size of $\mathcal{S}_n$. Analogously, even though the floating point solution does not fall into the hypothesis of Theorem 1.2, the stepsize h_{opt} is robust enough to handle the stability restriction. Noticing that n_{opt} is defined to satisfy $1/\varepsilon \leqslant e^{2(n_{\text{opt}}-1)}$ (see [JZ05]), the stepsize is bounded by

$$h_{\text{opt}} \leqslant \frac{1}{e^2} \cdot \left(\frac{\max\{1, \|\widehat{y}_0\|\}}{\varepsilon |\sigma|^{n_{\text{opt}}} / (n_{\text{opt}}!)} \right)^{1/n_{\text{opt}}} \leqslant \left(\max\{1, \|\widehat{y}_0\|\} \cdot e^{-2} \right)^{1/n_{\text{opt}}} \cdot \frac{1}{|\sigma|} \cdot (n_{\text{opt}}!)^{1/n_{\text{opt}}} \tag{15}$$

so, if $\|\widehat{y}_0\| \leqslant e^2$, it follows that $h_{\text{opt}}|\sigma| = \mathcal{O}(\ell_{n_{\text{opt}}})$. In fact, the condition $\|\widehat{y}_0\| \leqslant e^2$ can be weakened by appropriately choosing the absolute and relative errors of [JZ05]. For simplicity, in stiff problems, the stepsize could be simply modified by dividing it by $\|\widehat{y}_0\|^{1/n_{\text{opt}}}$.

Note that these bounds are based on asymptotic estimates and are satisfied for sufficiently large values of the order. For this very reason, stepsize control strategies include safety factors.

3.1.2 Stability through order increase

An alternative approach to the stability restriction $|s_n(h\sigma)| \leqslant 1$ is to use higher orders or precision without the need to reduce the stepsize. In particular, for fixed h and σ (large and negative), an estimate of the minimum order n for which $|s_n(h\sigma)| \leqslant 1$ is satisfied can be obtained by inverting a truncation of the asymptotic formula derived in Theorem 2.4. Note that multiplying by $2e$ and taking the exponential,

$$-h\sigma < \frac{n}{e} + \frac{1}{e} \log\left(\sqrt{2\pi n}(1+e)\right) \Leftrightarrow e^{-2eh\sigma} < e^{2n} 2\pi n (1+e)^2,$$

and dividing by $\pi(1+e)^2$, being both sides real and positive, we can take the principal branch of the Lambert W function (see [CGH+96, Lóc22]), which is strictly increasing for positive values, yielding

$$n > \frac{1}{2} W\left(\frac{e^{-2eh\sigma}}{\pi(1+e)^2} \right).$$

This restriction has several drawbacks, the first one being that the expression above grows roughly as $-eh\sigma$, rendering this approach impractical for highly stiff problems, where $-\sigma \gg 1$. In addition, the increase in order should be accompanied by an increase in precision, which could be chosen as per Theorem 1.2. Furthermore, the desired value of h has to be determined and σ has to be computed. A simple idea is to use a cheap implicit method to determine the desired stepsize in stiff regions and use automatic differentiation to compute the stiffness indicator on the go. Therefore, this option may only be of interest if such a high precision is actually required for the solution.

3.2 Higher order error terms

In the previous analysis, higher orders of ε could be considered in (9). Analogously, this would be the use of jet transport of 1 symbol and of the same order as that of the highest power of ε, being equivalent to the computation of the Taylor coefficients of the variational equations of that same order. However, for orders higher than one, the variational equations are linear but not homogeneous; that is, they are of the form

$$v'(x) = A(x)v(x) + b(x),$$

with initial condition $v(x_0) = 0$. Therefore, bounds like (4) should be derived for this case by appropriately extending the bound mentioned in [Söd06] for constant A,

$$\|v(x)\| \leqslant \frac{e^{x\mu(A)} - 1}{\mu(A)} \max_{x_0 \leqslant \tau \leqslant x} \|b(\tau)\|.$$

Let us also note that, given the recursive nature of the definition of the variational equations, if these were ill-behaved at a certain order, say m, they would appear as first order error terms in the computation with a floating point arithmetic of the variational equations of order $m-1$, in the same sense as the variational equations of order 1 appear in the computation of the solution of the IVP. By this principle, the effect of an ill-behaved high-order variational equation could affect the computation of the solution of the IVP. However, we have not explored this possibility in the present note.

4. Numerical experiments

The results in this section have been computed using an AMD Ryzen 5 processor running at 3.3 GHz, the GNU Compiler Collection 11.4.0, the `taylor` package 2.1 [GJZ22] and the MPFR library 4.1.0 [FHL+07] with GMP 6.2.1. As the `taylor` package has support for extended precision arithmetic through MPFR, we require the library to use a precision of $\lfloor d \log_2(10) \rfloor + 1$ bits, so to work with around d decimal digits. Therefore, by choosing the unit roundoff

$$u_d = 2^{-(\lfloor d \log_2(10) \rfloor + 1)},$$

we ensure $-\log_{10}(u_d) \geqslant d$. Some particular values used in this section are $u_{16} = 2^{-54} \approx 5.5 \times 10^{-17}$, $u_{100} = 2^{-333} \approx 5.7 \times 10^{-101}$, $u_{300} = 2^{-997} \approx 7.4 \times 10^{-301}$, and $u_{500} = 2^{-1661} \approx 9.7 \times 10^{-501}$. Both the order and stepsize of the Taylor method are chosen as per Theorem 1.2. For the values of the unit roundoff above, the values of n_{opt} are respectively $n_{\text{opt}}(u_{16}) = 20$, $n_{\text{opt}}(u_{100}) = 117$, $n_{\text{opt}}(u_{300}) = 347$ and $n_{\text{opt}}(u_{500}) = 577$. To study (9), ε is chosen equal to the unit roundoff and v_0 as the normalized vector of all ones. The stiffness indicator $\sigma(A)$ of (5) is taken as the sum and not the mean of $M(A)$ and $m(A)$, dropping some structural properties, as it seemingly captures better the behavior of $v(x)$ in these examples. All instances of a norm $\|\cdot\|$ in this section refer to the infinity norm $\|\cdot\|_\infty$, except for the computation of logarithmic norms, for which we prefer that induced by the euclidean norm $\|\cdot\|_2$.

4.1 The van der Pol oscillator

Let us first consider the van der Pol oscillator (VDPOL),

$$\begin{aligned} y_1' &= y_2, \\ y_2' &= \mu(1 - y_1^2)y_2 - y_1, \end{aligned}$$

with initial conditions $y(0) = (2, 0)$. As the stiffness of the VDPOL increases with the parameter μ, we fix $\mu = 100$, for which the problem is already stiff. Having a unique limit cycle with period close to 1.6μ for μ large [SJC15], we consider the problem on the interval $[0, 2\mu]$. We use as unit roundoff u_{100}.

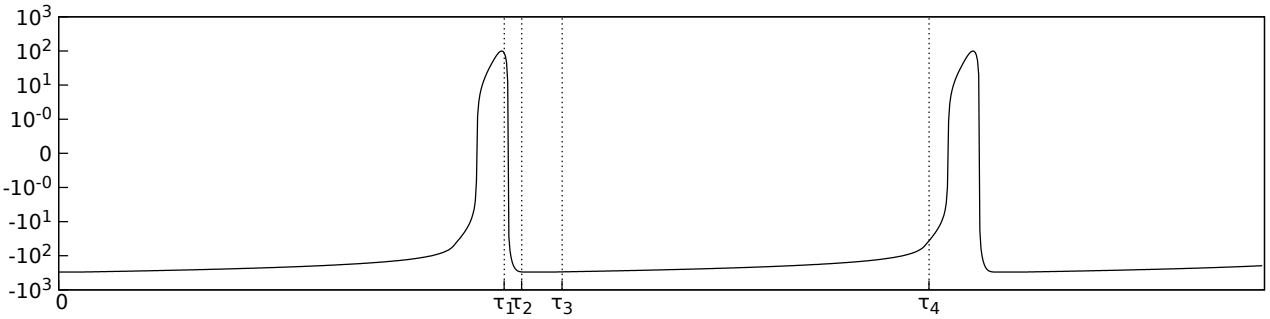

Figure 3: *Stiffness indicator of the VDPOL for* $\mu = 100$. The panel (symlog_{10} scale) shows $\sigma(\mathrm{D}_y f(x, y(x)))$ w.r.t. the stepsize in Figure 5. The horizontal axis shows the studied points $\tau_1, \ldots, \tau_4$.

To analyze the Taylor method along the solution, we study its behavior at the representative times $\tau_1 \approx 81.176$, $\tau_2 \approx 81.201$, $\tau_3 \approx 82.690$, and $\tau_4 \approx 159.386$, marked in the figures. As it can be seen in Figure 3, the stiffness indicator is large at all τ_i, but it is only positive at τ_1, where there is no stiffness. In fact, at τ_1, the Taylor coefficients are characterized by their rapid growth, indicating a reduction in the radius of convergence, which is reflected in the stepsize shown in Figure 5. In Figure 5 we also see that there is no effective order reduction, and in Figure 4 that neither condition (11) nor (12) holds. Being the stiffness indicator negative at τ_2, one would expect stiffness, but as seen in Figure 4, the behavior of the coefficients $\{{y_0}^{[k]}\}_k$ is analogous to that at τ_1. This may be caused by the fact that, despite the strong stiffness (note that the minimum of $\sigma(\mathrm{D}_y f(x, y(x)))$ is close to $x = \tau_2$), the behavior is dominated by the reduced radius of convergence. We remark that this possibility is accounted in the estimator (14).

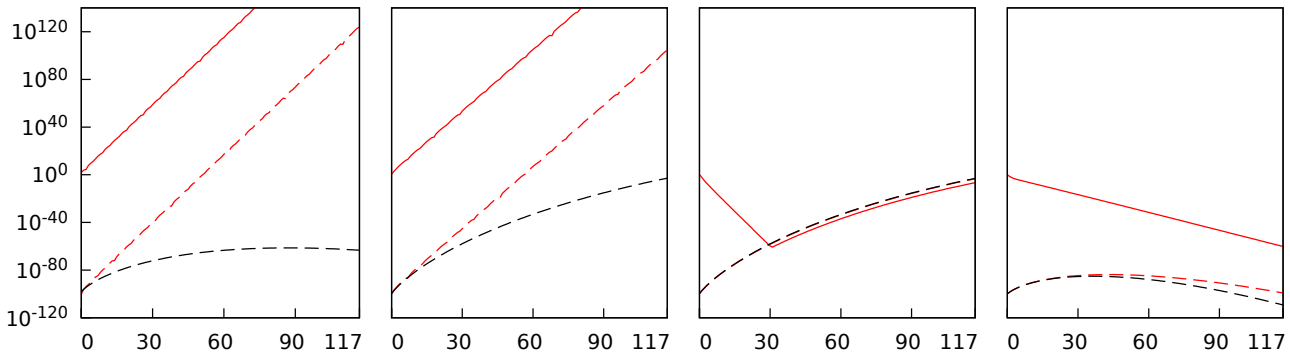

Figure 4: *Behavior of the coefficients of the Taylor method for the VDPOL with* $\mu = 100$ *and* $\varepsilon = u_{100}$. The panels ($\log_{10}$ scale) show for the distinct study points τ_1 to τ_4 the values $\|{y_0}^{[k]}\|$, $\varepsilon\|{v_0}^{[k]}\|$ and $\varepsilon|\sigma|^k/(k!)^{1/k}$ (from top to bottom in the first panel) with respect to the order k.

Lastly, we see in Figure 4 that, at τ_3 and τ_4, the coefficients decay fast (in τ_3 only up to some order) and the condition (12) is satisfied. The main difference is that, at τ_3, (11) holds and the effective error is reduced. This does not happen at τ_4, as can be seen in Figure 5. We can also see in this figure that the stepsize is restricted at τ_3 but it is not at τ_4 (this is reinforced by Figure 6). Therefore, the stiff region in this setting is approximately comprised between τ_3 and τ_4 (note that τ_3 is just inside and τ_4 is just outside), and the analogous on the rest of the solution (recall the periodic orbit and notice its symmetry). An analysis of the behavior of the points in this region is analogous to that of τ_3.

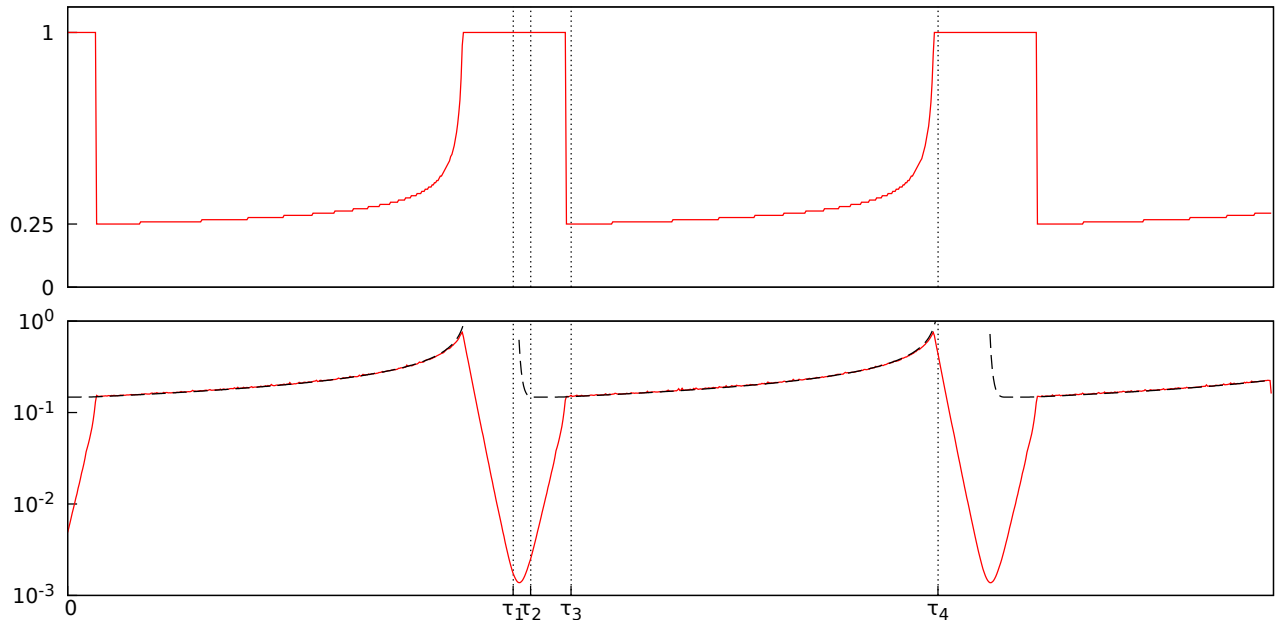

Figure 5: *Order and stepsize attained for the VDPOL with* $\mu = 100$ *and* $\varepsilon = u_{100}$. The first panel (linear scale) shows the ratio $n_{\text{opt}}/n_{\text{eff}}$. The second panel ($\log_{10}$ scale) shows the stepsize h_{opt} of the Taylor method of order n_{opt} (solid) and the value $(n_{\text{opt}}!)^{1/n_{\text{opt}}}/|\sigma|$ (dashed), demonstrating (14).

Regarding the stepsize restrictions discussed in Section 3.1.1, we show in Figure 5 how the stepsize control naturally ensures the stability of the integration step by satisfying (15). In Figure 6, we illustrate the discussion in Section 3.1.2 that an appropriate increase in precision and order reduces stepsize constraints, thus improving the behavior of the Taylor method. In particular, we see how bad this restrictions are when choosing $\varepsilon = u_{16}$, which is close to the precision used by the `double` arithmetic. Note that for u_{16}, $n_{\text{opt}} = 20$, so the effective order n_{eff} is 3 at its lowest, as seen in Figure 6.

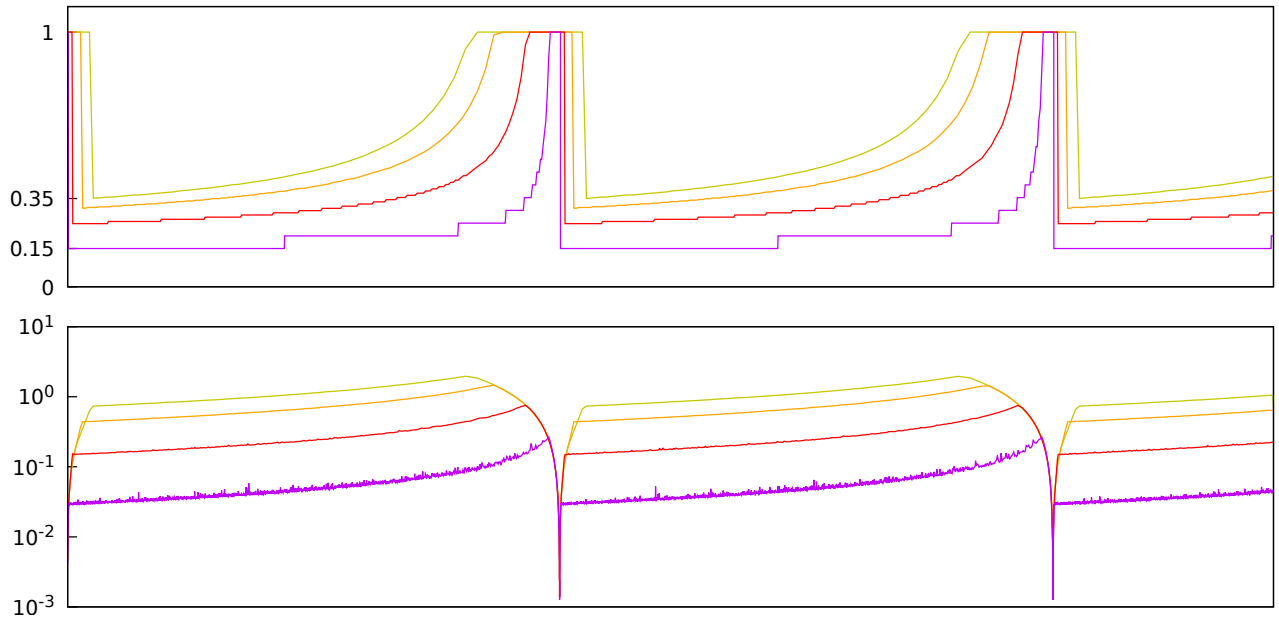

Figure 6: *Restrictions on the order and stepsize of the VDPOL with* $\mu = 100$ *and distinct* ε. The first panel (linear scale) shows the ratio $n_{\text{opt}}/n_{\text{eff}}$ with ε being $u_{500}, u_{300}, u_{100}, u_{16}$ from top to bottom. The second panel ($\log_{10}$ scale) shows the stepsize of the Taylor method with ε chosen as in the first panel. Both panels are with respect to time.

4.1.1 Extended precision computations

Given the improvement in the behavior of the Taylor method when using extended precision, we have computed the amplitude and period of the limit cycle of the VDPOL for increasing values of μ to 100 significant digits. To compute the period of the orbit, we use the Poincaré section $\Sigma = \{y_2 = 0\}$ (a Newton method is required to land on Σ). One way to compute the fixed point on Σ is to proceed as described in [GJJ+23], using jet transport of order 1 and 1 symbol to compute the Poincaré map and its derivative. This is used to perform iterations of a Newton method to find the fixed point. However, as noted in [Amo22], the strong attraction of the periodic orbit for large values of μ allows the determination of the fixed point without need of this approach. As it also is mentioned in [Amo22], given the symmetry of the periodic orbit, only half a period (first return time to Σ) is needed. In Table 1 we report the computing times for distinct precision u_d and for some representative values of μ for which the derivative of the Poincaré map is not needed, so that the computing time is comparable.

Table 1: *Computing time (in seconds) for the period and amplitude of the VDPOL for distinct values of* μ *and precisions* u_d.

μ	u_{100}	u_{300}	u_{500}
100	0.744055	6.811759	28.999913
200	2.514231	18.957733	66.016140
300	5.390844	39.762842	126.921753
400	9.410912	65.557191	211.368813
500	14.509931	97.135631	314.735245

As an example, we focus on the computation using as unit roundoff u_{100} and report the values of the amplitude and period in Tables 2 and 3. However, to provide only correct digits, their computation is verified and corrected with a much higher precision. Therefore, as detailed in the tables, the first corrected digit is marked with an underline. We remark that these quantities were first computed by Amore [Amo22], where 400 digits and 201 Taylor coefficients were used in his Padé approximant of order $[100, 100]$. Note that being the Padé approximant diagonal, the method should be A-stable, as proved by Varga (see [Ehl73]), but the behavior of the stepsize reported in [Amo22, Figure 7] is close to that of the Taylor method, as seen in Figure 7. In Tables 2 and 3 we also mark with a light red box the first non-coincident digit with these results.

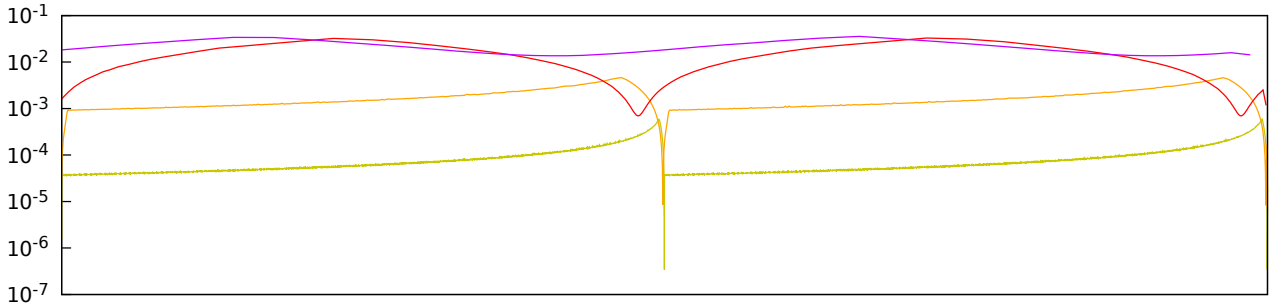

Figure 7: *Stepsize attained for the VDPOL with different μ and $\varepsilon = u_{100}$.* The panel ($\log_{10}$ scale) shows the stepsize of the Taylor method of order n_{opt} divided by the period with μ being 1, 10, 100, 500 from top to bottom with respect to time normalized by the period.

4.2 The Oregonator model

Let us briefly study the Oregonator model (OREGO),

$$\begin{aligned} y_1' &= s(y_1 - y_1 y_2 + y_2 - q y_1^2), \\ y_2' &= (y_3 - y_2 - y_1 y_2)/s, \\ y_3' &= w(y_1 - y_3), \end{aligned}$$

with initial conditions $y(0) = (1, 1, 2)$ and parameters $s = 77.27$, $q = 8.375 \cdot 10^{-6}$, $w = 0.161$. As it has a limit cycle with period close to 302, the solution is studied in the interval $[0, 320]$. This is the same setting as in [SJC15]. We use as unit roundoff u_{100}.

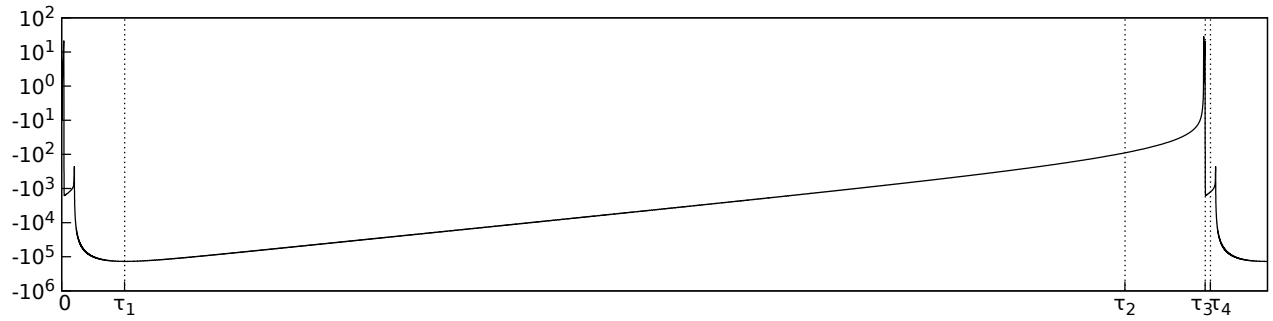

Figure 8: *Stiffness indicator of the OREGO.* The panel (symlog_{10} scale) shows $\sigma(\mathrm{D}_y f(x, y(x)))$ w.r.t. time. The horizontal axis shows the study points $\tau_1, \ldots, \tau_4$.

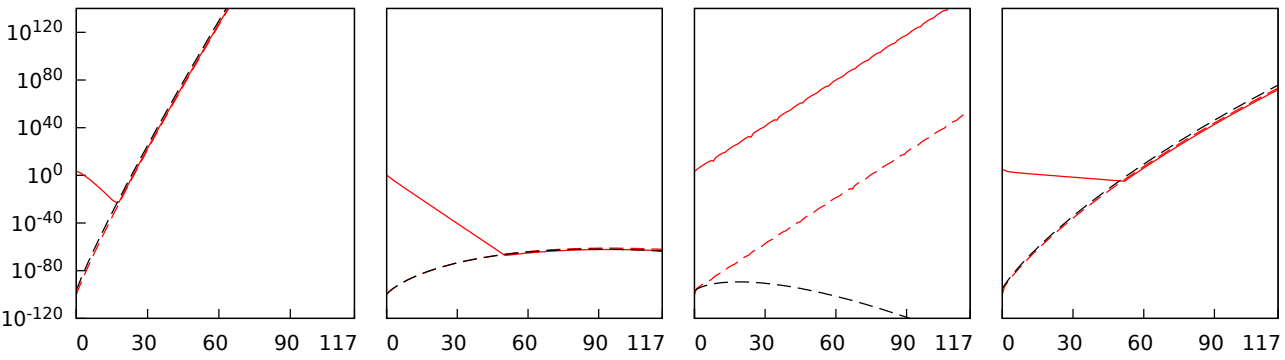

Figure 9: *Behavior of the coefficients of the Taylor method for the OREGO with $\varepsilon = u_{100}$.* The panels ($\log_{10}$ scale) show for the distinct study points τ_1 to τ_4 the values $\|{y_0}^{[k]}\|$, $\varepsilon\|{v_0}^{[k]}\|$ and $\varepsilon|\sigma|^k/(k!)^{1/k}$ (from top to bottom in the third panel) with respect to the order k.

Analogous to the study of the VDPOL, we show the behavior of the Taylor method for the OREGO at some representative times $\tau_1 \approx 16.689, \tau_2 \approx 282.170, \tau_3 \approx 303.435, \tau_4 \approx 304.822$. Figure 8 shows larger

negative values of the stiffness indicator of the OREGO when compared to those of the VDPOL in Figure 3. This fact is reflected in the coefficients shown in Figure 9, where the growth of the error terms is much faster. This is also visible in Figure 10, as the restrictions on the effective order and stepsize are stronger. In particular, by comparing this figure with Figure 5, we observe that the effective order n_{eff} reaches a minimum of 16 for the OREGO while of 29 for the VDPOL (recall $n_{\text{opt}}(u_{100}) = 117$).

Although the behavior of the solution of the OREGO is in some sense more complex than that of the VDPOL, an analysis of the Taylor method yields similar behaviors. In particular, as for the VDPOL, the coefficients in Figure 9 are well represented by (11) in stiff regions, and the second panel of Figure 10 demonstrates that the stability restriction on the stepsize studied in (14) is satisfied.

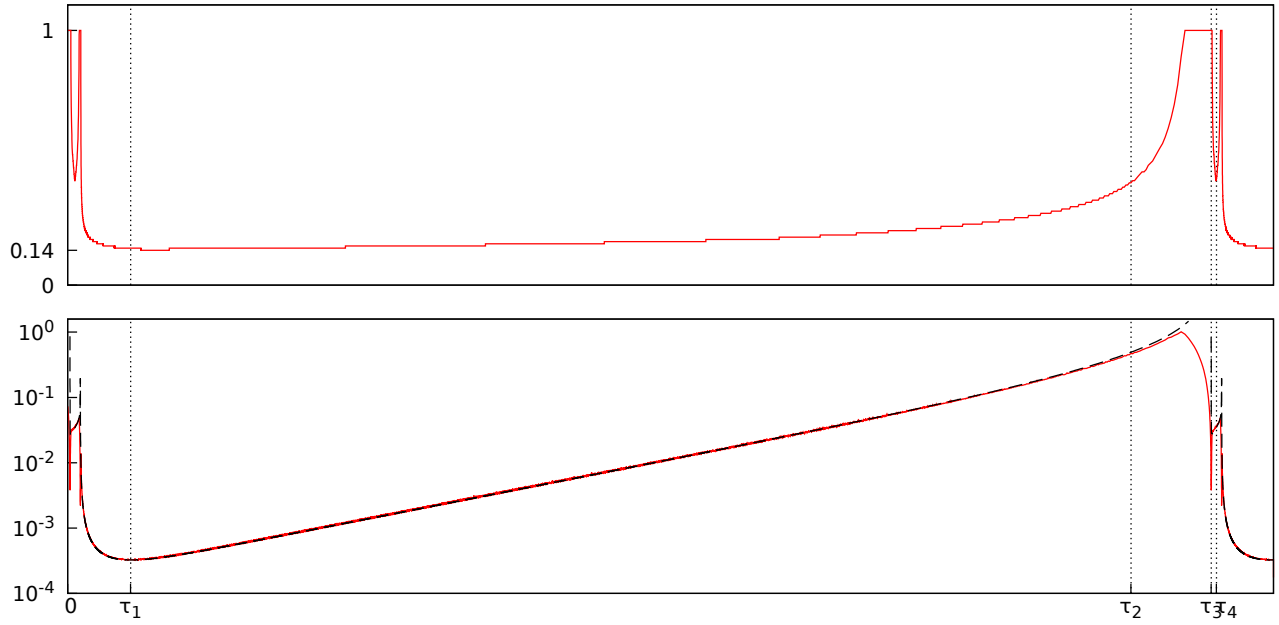

Figure 10: *Order and stepsize attained for the OREGO with* $\varepsilon = u_{100}$. The first panel (linear scale) shows the ratio $n_{\text{opt}}/n_{\text{eff}}$. The second panel ($\log_{10}$ scale) shows the stepsize of the Taylor method (of order n_{opt}) (solid) together with the value $(n_{\text{opt}}!)^{1/n_{\text{opt}}}/|\sigma|$ (dashed), demonstrating the restriction (14). Both panels are with respect to time.

5. Conclusions

First, the boundary of the stability region $\mathcal{S}_n$ of the Taylor method has been analyzed through the partial sums of $\exp(z) - \alpha$, whose zeros were already studied by Dieudonné. The ideas of Szegő *et al.* for the zeros of the partial sums of $\exp(z)$ allow to derive an explicit formula for the asymptotic growth of $\mathcal{S}_n$ with respect to the order of the Taylor method.

We have then focused on the phenomenon of stiffness and, in particular, on the recently developed stiffness indicator of Söderlind *et al.* [SJC15]. This indicator characterizes the behavior of the variational equations of the solution which, for our purpose, serves as the error of the floating point coefficients of the method. Stiffness seemingly appears when these errors dominate the behavior of the solution, reducing the effective order of the method. Nonetheless, these perturbed coefficients can still be used by paying the price of stepsize restrictions. That is consistent with the fact that usual stepsize control strategies do not increase the error of the method by appropriately reducing the stepsize. Alternatively, if high precision computations are desired, a suitable increase in the order of the method and in the precision of the arithmetic will reduce the restrictions on the stepsize. Therefore, when extended precision is required, letting aside the additional work of the arithmetic, a better performance of the Taylor method is expected. This is a consequence of the fact that the stiffness indicator "is exclusively a problem property, independent of the choice of integration method" [SJC15], so it is, in particular, unaffected by the choice of the order of the Taylor method.

The asymptotic formula for the growth of $\mathcal{S}_n$ derived in Section 2 allows to analyze the stability of some stepsize control strategies, and is used to construct a lower bound on the order of the Taylor method for which a given stepsize is stable. These restrictions of the method have been studied in the numerical experiments of Section 4 for the van der Pol and the Oregonator problems. As an example, we have computed 100 significant digits of the period and amplitude of the van der Pol oscillator. The results are compared with those of [Amo22] where Padé approximants are used. It seems that a traditional Taylor method with the previous considerations can deliver a better accuracy.

Nevertheless, we stress that the conclusions on the behavior of the Taylor coefficients are mainly drawn on the study of the truncation error of the Taylor method. If the coefficients computed were used for other purposes, such as the determination of the coefficients of an implicit method (as an implicit Taylor, Hermite-Obreschkoff or Padé method; see [KC92, CGH$^+$97, Ned99, Amo22]), the consequences of these errors may differ and remain to be studied.

Acknowledgements

The project has been supported with the Spanish grant PID2021-125535NB-I00 (MICINN / AEI / FEDER, UE) and the Catalan grant 2021 SGR 01072. The project that gave rise to these results also received the support of the fellowship from "La Caixa" Foundation (ID 100010434), the fellowship code is LCF/BQ/PR23/11980047. This work has been also funded through the Severo Ochoa and María de Maeztu Program for Centers and Units of Excellence in R&D (CEX2020-001084-M).

Statements and Declarations

The authors declare no conflict of interests.

References

[ABBR12] Alberto Abad, Roberto Barrio, Fernando Blesa, and Marcos Rodríguez. Algorithm 924: TIDES, a Taylor Series Integrator for Differential EquationS. *ACM Transactions on Mathematical Software*, 39(1):1–28, November 2012.

[Amo22] Paolo Amore. Computing the solutions of the van der Pol equation to arbitrary precision. *Physica D: Nonlinear Phenomena*, 435:133279, July 2022.

[BBL05] Roberto Barrio, Fernando Blesa, and Martin Lara. VSVO formulation of the Taylor method for the numerical solution of ODEs. *Computers & Mathematics with Applications*, 50(1-2):93–111, July 2005.

[CC82] George Corliss and Y. F. Chang. Solving ordinary differential equations using Taylor series. *ACM Transactions on Mathematical Software*, 8(2):114–144, June 1982.

[CGH$^+$96] Robert M. Corless, Gaston H. Gonnet, D. E. G. Hare, David J. Jeffrey, and Donald E. Knuth. On the Lambert W function. *Advances in Computational Mathematics*, 5(1):329–359, December 1996.

[CGH$^+$97] George F. Corliss, Andreas Griewank, Petra Henneberger, Gabriela Kirlinger, Florian A. Potra, and Hans J. Stetter. High-order stiff ODE solvers via automatic differentiation and rational prediction. In Gerhard Goos, Juris Hartmanis, Jan Leeuwen, Lubin Vulkov, Jerzy Waśniewski, and Plamen Yalamov, editors, *Numerical Analysis and Its Applications*, volume 1196, pages 114–125. Springer Berlin Heidelberg, Berlin, Heidelberg, 1997.

[Cha89] Y.F. Chang. Solving stiff systems by Taylor series. *Applied Mathematics and Computation*, 31:251–269, May 1989.

[Chr92] Bruce Christianson. Reverse accumulation and accurate rounding error estimates for Taylor series coefficients. *Optimization Methods and Software*, 1(1):81–94, January 1992.

[Cop65] William A. Coppel. *Stability and Asymptotic Behavior of Differential Equations.* Boston, Heath, March 1965.

[Die35] Jean Dieudonné. Sur les zéros des polynomes-sections de e^x. *Bulletin des Sciences Mathématiques*, 70:333–351, 1935.

[Ehl73] Byron L. Ehle. A-Stable methods and Padé approximations to the exponential. *SIAM Journal on Mathematical Analysis*, 4(4):671–680, November 1973.

[FHL+07] Laurent Fousse, Guillaume Hanrot, Vincent Lefèvre, Patrick Pélissier, and Paul Zimmermann. MPFR: A multiple-precision binary floating-point library with correct rounding, `https://www.mpfr.org/`. *ACM Transactions on Mathematical Software*, 33(2):13, June 2007.

[For23] Philip P. Forrier. Jet transport for General Linear methods. Master's thesis, Universitat de Barcelona, June 2023.

[GG14] Robert B. Gardner and Narendra K. Govil. Eneström–Kakeya theorem and some of its generalizations. In Santosh Joshi, Michael Dorff, and Indrajit Lahiri, editors, *Current Topics in Pure and Computational Complex Analysis*, pages 171–199. Springer India, New Delhi, 2014.

[GJJ+23] Joan Gimeno, Àngel Jorba, Marc Jorba-Cuscó, Narcís Miguel, and Maorong Zou. Numerical integration of high-order variational equations of ODEs. *Applied Mathematics and Computation*, 442:127743, April 2023.

[GJZ22] Joan Gimeno, Àngel Jorba, and Maorong Zou. Taylor package, version 2, `http://www.maia.ub.es/~angel/taylor`, 2022.

[GKW12] Andreas Griewank, Kshitij Kulshreshtha, and Andrea Walther. On the numerical stability of algorithmic differentiation. *Computing*, 94(2-4):125–149, March 2012.

[HW96] Ernst Hairer and Gerhard Wanner. *Solving Ordinary Differential Equations II*, volume 14 of *Springer Series in Computational Mathematics*. Springer Berlin Heidelberg, Berlin, Heidelberg, 1996.

[JZ05] Àngel Jorba and Maorong Zou. A software package for the numerical integration of ODEs by means of high-order Taylor methods. *Experimental Mathematics*, 14(1):99–117, January 2005.

[KC92] Gabriela Kirlinger and George Corliss. On implicit Taylor series methods for stiff ODEs. In *Computer Arithmetic and Enclosure Methods*, pages 371–379. Elsevier Science Publishers B.V., Oldenburg, 1992.

[KLK15] David Ketcheson, Lajos Lóczi, and Tihamér A. Kocsis. On the absolute stability regions corresponding to partial sums of the exponential function. *IMA Journal of Numerical Analysis*, 35(3):1426–1455, July 2015.

[Lóc22] Lajos Lóczi. Guaranteed- and high-precision evaluation of the Lambert W function. *Applied Mathematics and Computation*, 433:127406, November 2022.

[Ned99] Nedialko S. Nedialkov. *Computing Rigorous Bounds on the Solution of an Initial Value Problem for an Ordinary Differential Equation.* PhD thesis, University of Toronto, 1999.

[Nem10] Gergő Nemes. New asymptotic expansion for the Gamma function. *Archiv der Mathematik*, 95(2):161–169, August 2010.

[RB12] Marcos Rodríguez and Roberto Barrio. Reducing rounding errors and achieving Brouwer's law with Taylor series method. *Applied Numerical Mathematics*, 62(8):1014–1024, August 2012.

[Ros42] Paul C. Rosenbloom. *On Sequences of Polynomials: Especially Sections of Power Series.* PhD thesis, Stanford University, 1942.

[Sim01] Carles Simó. Global dynamics and fast indicators. In Bernd Krauskopf, Henk Broer, and Gert Vegter, editors, *Global Analysis of Dynamical Systems.* Taylor & Francis, June 2001.

[SJC15] Gustaf Söderlind, Laurent Jay, and Manuel Calvo. Stiffness 1952–2012: Sixty years in search of a definition. *BIT Numerical Mathematics*, 55(2):531–558, June 2015.

[Söd06] Gustaf Söderlind. The logarithmic norm. History and modern theory. *BIT Numerical Mathematics*, 46(3):631–652, September 2006.

[Var12] Antonio R. Vargas. Zeros of sections of some power series. Master's thesis, Dalhousie University, September 2012.

[Zem05] Stephen M. Zemyan. On the zeroes of the N-th partial sum of the exponential series. *The American Mathematical Monthly*, 112(10):891–909, December 2005.

Table 2: *Period of the VDPOL for distinct μ computed with the Taylor method using $\varepsilon = u_{100}$ and order n_{opt}.* Underlines mark the first digit corrected with a higher precision computation. Light red boxes mark the fist digit that differs from the results in [Amo22].

μ	T
1	6.6632868593231301896996820304823287068126463168838766551148631820809258648456068648689666200532712233
10	19.0783695669390140704301128258151723269495091319495515726558065684382450533127411577338871600711224 6
20	34.6823233116526835671200001106804324139956033545207539798396425595322081483315148141784355174104814 2
30	50.5436864827405120702827386466837046838248278586073506538947527935622292695766290244208606263817521 0
40	66.5013690428044769896971924943387837598438117282074868545719371591498846551325086349475619985599821 2
50	82.5083338932307821868333686974998745937405908586186277867538544102124003517095023264804783738749969 4
60	98.5447889588789034118236568301952218695801665044095231251659545600429935330665056316491071515057152 5
70	114.6006663004441624691712023317540856185451162034576279580190523911294876452269860606383216961761215
80	130.6701966309285473096077258773381797819703833326686760165963074383845409405823897922106445547563428
90	146.7497896543084106513374421250368854262190114879122183612587391565662535580686126367442628577020043
100	162.8370710923700121324637071671686166801818391038559611357666728540226928276371599901787833110252564
110	178.9303956907033679871688310695657159323417168135937922472711936862634798797065910073778443003100491
120	195.0285802556076526910160058643286113856413040774148397015025046291085887859870658756179389085971796
130	211.1307477804160260130832331863590232741382508015255437999265521274563460940912363700317134456024905
140	227.2362316910533012521444863792345519317926635296215340947212434470538699636331704863156601505403006
150	243.3445145087953931135502082098788891571273471387131884042823631594633493846569879423539468834013124
160	259.4551871552089954913517277272206473199985957741243565799737323251409484803982037303780223559037179
170	275.5679211327523211576511486355320960580031645969284306833900520902209914645207652127999437789348207
180	291.6824490104429176636024212529204140524163494516962540912121426736499348947208292897874488332050626
190	307.7985504241069457922015591780920378614606316407770889761198474674473028851653136541693381088651135
200	323.9160418323323196052744334743514572330591352304211850032764200605474695617827325555219016088358064
210	340.0347688806522434904435134601326736951700147373448939769902487386940575712459682079110500234187 17
220	356.1546006684104003067298586327525331982255704647101679116821495869556226155397898225319264506440639
230	372.2754252482098363564602268458485149789880169166789785925357810440972561748225119598807497831772815
240	388.3971462610618011013038198916975395522677722189419414224652127005211074077504912273720584228538532
250	404.5196801965184163871870483252417534129149893308985855734118257674185692704093695250596637461397278
260	420.6429542534117152872015862950200327148950773405052472443498537114242041539084627577505562882057569
270	436.7669046183784061997777264506815647938055223685815973519157893021809412437496513849994688098179346
280	452.8914750730853333239771225564670217954080152594118401826623836805454265359833714379551739495594770
290	469.0166158581516320832875103415375882683397513540431583325719881015948320585564394337012616182121934
300	485.1422827394258644411994738128162929528511728967565610619365505973036022082905924814438907274623181
310	501.2684362351727278043262197886224674534152153985523980152199838682809188502353717678108534815970037
320	517.3950409722499517962169558534433819784295128655886321961149836442728358619817664738133788941608834
330	533.5220651464685439093770993809975226199501092612890489460184777692815090361258658346616492522214782
340	549.6494800676934839949154867656319140696297368261640221561901546724731094473412552942021120600295546
350	565.7772597743251395754584188044891972324418362059662852878315745165859164044732587939661024391173550
360	581.9053807049371611599899409528464197025076079369324177055544818049076752372353891929765193185005965
370	598.0338214172741708554742746438097871784657137100509247412814597229030965656398052260558356361461 46
380	614.1625623467065316667294887459766934907192942444561368480601789297721379562415973388864555874719770
390	630.2915855977279002588325318270425179584336562242802573981195152721692507775054721404596139389248300
400	646.4208747632589801817235754087546670050667520695370442192859197917172073891282189403517007231230742
410	662.5504147674587935472268172823212596053856889929061113486650534518559143908813267950837851161107142
420	678.6801917284962811716715427761830037224858485711644890650826028465201225367955936105236738829300840
430	694.8101928383406651011117404415935456713454473520735101239397598381973576287877899582001546431305008
440	710.9404062571197622304402500844361021088511568057723287903810936635278920433865557252749603650692951
450	727.0708210199951894034096387862684901871433733460526811373298258977410795037769607991349266970698081
460	743.2014269548306432660248072532951912484203422142802006802759653947115260819969130621543319895466478
470	759.3322146091985929587520824066647575473765056190071596350044144396300656133940892613873589424075726
480	775.4631751854931013470343234244302326331407339369619665047832135462539340067800370265770753832435831
490	791.5943004831010125943528547313571368118302188840571420579003403211905738258438526069792889800922969
500	807.7255828467374855142099344594401073186279176290097708714275059764518206392913479642713530681050943

Table 3: *Amplitude of the VDPOL for distinct μ computed with the Taylor method using $\varepsilon = u_{100}$ and order n_{opt}.* Underlines mark the first digit corrected with a higher precision computation. Light red boxes mark the fist digit that differs from the results in [Amo22].

μ	A
1	2.008619860874843136509640188362640366192026137720714461127703247615558726584991155953057790709097764
10	2.014285360926405285327639819151920183122053633536581375785514775840505595191629394412431198122197533
20	2.007789970865430297274867350090457336303719272622512696580222467839163820644590094385995046731852068
30	2.005164254840654557051777186680049721988490763259078944821305865733440807262686417365186060483853802
40	2.003789381619443789571203145287844923089135343779111957674707624353600707572222969176109242784488703
50	2.002955933757648402826109718945871764979914720146069491639268919228280941255065893414456892214808004
60	2.002401919063881473920962090208714663235156271998258030687422113141268600481080681056348881636454034
70	2.002009596082639609289697462083514119112813772856077413775296699647238878049627998777911871776993942
80	2.001718652710708668905375467432853701724717282116218318894524355022607543603472606814812673333891300
90	2.001495168861862908252915078070973635620733425887828025607985838234406501535795329520921218813904854
100	2.001318681177224161237412765674824826667922262552186082947860663645944718541257075874824291065133597
110	2.001176150664201236511554898162392329309803631919700088396165021635090622731953166376363185345190467
120	2.001058896554125927029392927438080919331098636531505741935700786658637918519040964812470011465259065
130	2.000960927844888534197421329197213513163533964064997696319356875362523084014342159495491081566374532
140	2.000877983652867070899563966628262022269236536408068634986331923205730266248081399764040778573457872
150	2.000806955271625817278643513939997236295393278928069489496739293779680272206361514498205112393886658
160	2.000745524338127997986533399402526338459501029215022413403802471156496719380286552841303498699166454
170	2.000691928650507049010444693810276888632234923699748845764204325369807162600992668870049753693914348
180	2.000644806183587289954560918219707872421639629764757465033098886830120895062335564168746005183167098
190	2.000603088546078420297503695261372256400644888894879382845043708598328299403205400741349039400898667
200	2.000565926576760211522417824772932917267562790191698912402919850289563593680876332599753138742066904
210	2.000532637350753826167807899544044099402616675472884782815702328994100650744957001382965323763051867
220	2.000502665763518248325354257921241551809517650968823097692036278979440318254163946014190489411599806
230	2.000475556236848568636954324017185605467137320938779282327081023791577576731757080734492140855109316
240	2.000450931578303478694537510744220248976114354365642128210382176047146010114604394305189436058795740
250	2.000428476977723451850290406957396326497015626299411770298015994651998501623433226464531941204000360
260	2.000407927747058093988748823717862181612795541998090284257389144325547078829092172149764902564719008
270	2.000389059824524017306726894783981061575986906859073578895751544091178277158764196260296966014246 28
280	2.000371682345317609157227907905005606795933433938383565745122081496027981775545646109723946722435718
290	2.000355631774790119931882114768567816619242450522793582699291719911732054675995403444109331703946892
300	2.000340767235358440381118336572999553385449901440431020937886115010068300706803207636643738494352265
310	2.000326966754318491752882158288726666347822269174555888819685335381219042241539507445589914126673444
320	2.000314124228514365047590787480224800388011045630717020905323049774289130633510670020231543638910683
330	2.000302146951734816161384032376729083130293740082412165493512016110882487677683585416959621768557525
340	2.000290953587329248234887345448502018306154097277200952370316129354246338636069275694592131936921866
350	2.000280472495673520147801804304281450222834146751154194402383792845458390614590018139282388728999712
360	2.000270640346418482727432796549274334807090723809457625301021912279926785202157716023007066231316421
370	2.000261400960778407272014150919879490328851961702490111973205517604442731436470785107417568540835795
380	2.000252704340780169883024954575103776332039887880106187365966367674615954233486090162339825153616660
390	2.000244505851341729254186335289587647349025191125715300019568047920146842751944312158719222365729242
400	2.000236765527963692701424636298007565995335294141201369885707909024705207984905021905264276738379988
410	2.000229447488199892183365006648765079361335769644477289898322145200717840904979655958241132298599 34
420	2.000222519429289704999922115937529332436405089602733553210761715084325381901726400712785896716822217
430	2.000215952197659532174091044980369619020676193843196225450138050837614077484865400111102223006344027
440	2.000209719418637855073353468847162792740151388072266145846231279294924400850726940839455543996263234
450	2.000203797176831785484489994634091962887707480896472133778935604952800033427160310778667536166160719
460	2.000198163739300046960156775279678371962466920303239147813726832400200911102449590548664241320247353
470	2.000192799315017326821486381385659974607662167180381990234008789939302452667675207378354149880642 89
480	2.000187685845226716315931997510390663860906566981771710897933276683167515206752217716063468330289276
490	2.000182806820173743333076404516509646425847607747067792646395379556093756846055335211666721602593031
500	2.000178147118448723671856525505949565588507795231205946274908215891589873833904374812071090873502129